Inelastic resonant tunneling in C_{60} molecular junctions

Nikolai Sergueev,[1] Alexander A. Demkov,[1] and Hong Guo[2]

[1]*Department of Physics, The University of Texas at Austin, Austin, Texas 78712, USA*
[2]*Centre for the Physics of Materials and Department of Physics, McGill University, Montréal, Québec, Canada H3A 2T8*

We present an *ab initio* theory of inelastic electron tunneling spectroscopy along with the theoretical analysis of recent experiments on inelastic transport in molecular tunneling junctions involving C_{60} molecule. We present a self-consistent procedure for calculating electron charge density and tunneling current in the presence of the electron-phonon interaction. We find that electron tunneling is significantly influenced by several specific vibrational modes. Inelastic scattering suppresses resonance transmission peak and substantially redshifts the peak position. We investigate the microscopic origin of this behavior by calculating the relevant vibrational modes and resonance wave functions under nonequilibrium transport conditions.

PACS number(s): 73.63.−b, 68.37.Ef, 72.10.−d, 81.07.Nb

Understanding charge transport in molecular tunnel junctions (MTJ's) is a major problem of single molecule science. When a steady-state current is driven through a metal-molecule-metal (MMM) structure by an external bias voltage, the value of the current is influenced by many microscopic details of the system. It is generally expected that electron-phonon (e-p) interaction plays a vital role[1–4] in transport. Here, "phonon" refers to quantized molecular vibrational modes which couple to scattering states that traverse the device. These modes can be triggered by current even at low temperature (if the bias voltage is sufficiently large), inducing various effects in molecular devices such as atomic rearrangements and structural changes, and may be responsible for the heat dissipation. Experimentally, detection of single molecule vibrations in a transport measurement is a major challenge. The inelastic tunneling spectroscopy (IETS) is a powerful tool with spectroscopic sensitivity sufficient for identifying individual vibrations of a single molecule.[1–4] However, since the signal is not a direct measurement (second derivative of the current with respect to bias voltage), one needs a theoretical model to interpret the results.[5–7] Unfortunately, a comprehensive *ab initio* theory of e-p interaction in molecular transport has not been satisfactory established.[8,9]

The quantitative analysis of e-p effects for realistic devices requires atomistic first-principles calculations.[10–14] A particularly difficult theoretical challenge is to *quantitatively* analyze phonon effects for molecular devices during nonequilibrium quantum transport, i.e., during current flow, without any phenomenological parameters. In this case, it is necessary to calculate vibrational spectra, electron-phonon coupling, and its effect on the charge flow, in a self-consistent *nonequilibrium* formalism. At present, a very useful formalism is the density-functional theory (DFT) carried out within the Keldysh nonequilibrium Green's function (NEGF) framework.[15] In the NEGF-DFT formalism, the device Hamiltonian and electronic structure are determined by DFT, the nonequilibrium quantum statistics of the device is determined by NEGF, and electron-phonon effects are included self-consistently.[13,14] The role of self-consistency is twofold. The first is its appearance in the relationship between the electronic Green's function and e-p self-energy. Brandbyge and co-workers[13,14] implemented this in a self-consistent Born approximation. The second, and in our opinion the more important, is its appearance in the relationship between the electronic Green's function, electron charge density, and electronic Hamiltonian. This second self-consistency is absolutely necessary in the theory of IETS because the e-p coupling changes under current flow and thus depends on nonequilibrium physics.[16]

Unlike previous theoretical attempts reported to date,[13,14] in our theory of IETS we seek self-consistency between the device Hamiltonian including the e-p potential, NEGF, and phonon self-energy, while calculating phonon modes at nonequilibrium. We suggest that this is a crucial step in order to correctly obtain physical quantities such as electron density and tunneling current with the phonons included. This theory allows us to treat electrons and molecular vibrations on equal footing and calculate (i) electron density, (ii) vibrational spectrum, (iii) e-p coupling, and (iv) elastic and inelastic transmission coefficients and current. We use our theory to simulate IETS of metal-C_{60}-metal MTJ. C_{60} is one of the best studied molecules, and is commonly used experimentally[5,6,17,18] as a model system that is far beyond trivial and yet theoretically tractable. We find that for C_{60} contacted by Al leads, quantum transport is resonance mediated and electron tunneling is significantly affected by strong e-p coupling. Since the work function of most metals is substantially less than the ionization potential of C_{60}, qualitatively similar charge transfer from metal to the lowest unoccupied molecular orbital (LUMO) states of C_{60} is expected for many different metal leads.

We begin by briefly outlining our inelastic NEGF-DFT formalism. For a two-probe MMM device under bias V_b, its electron density matrix and Kohn-Sham Hamiltonian are first calculated self-consistently within NEGF-DFT.[15,16] The *elastic* transport properties (no e-p interaction) are obtained by the NEGF-DFT (Refs. 15 and 19) together with the total energy $E(\{\mathbf{R}_i\}, V_b)$ of the device scattering region. Here, $\mathbf{R}_i$ is the coordinate of atom labeled i (see Fig. 1). Next, we calculate vibrational frequencies ω_ν, with ν the mode index, and vibrational eigenvectors $\mathbf{e}_\nu$ by diagonalizing the dynamical matrix which is the second derivative of $E(\{\mathbf{R}_i\}, V_b)$ with respect to $\mathbf{R}_i$. Since $E(\{\mathbf{R}_i\}, V_b)$ is evaluated by NEGF-DFT at nonequilibrium during steady-state current flow, ω_ν ob-

tained this way reflects the nonequilibrium physics,[20] as discussed in Ref. [16]. The strength of the e-p interaction is given by a coupling matrix which is contributed to by all the relevant vibrational modes. Using ω_ν and $\mathbf{e}_\nu$, e-p coupling matrix g^ν can be obtained by standard formulation.[16]

A "full" theory describing the e-p interaction should include the following ingredients: from the electronic Hamiltonian, one computes phonons; from the phonons, a new electronic Hamiltonian is determined; and the process is iterated by NEGF-DFT until self-consistency. Unfortunately, this is computationally prohibitive for realistic device simulations. Instead, we proceed in three steps: (i) we calculate phonons by NEGF-DFT at nonequilibrium from the electronic Hamiltonian without including the e-p interaction; (ii) with these phonons, we compute e-p self-energy from electronic Green's function, this self-energy provides an e-p potential to the electron Hamiltonian that gives a new electronic Green's function, and this process is iterated to self-consistency; (iii) finally, we calculate transport properties including inelastic transmission coefficients and inelastic current. Compared with the full theory, our approximation lies in fixing the nonequilibrium phonon physics in step (i) without further e-p renormalization during the self-consistent iteration thus considering only first-order phonon processes.

After the inelastic NEGF-DFT is iterated to self-consistency, we calculate the total current,[19]

$$I_{L/R} = \frac{e}{h} \int dE\, \mathrm{Tr}[\Sigma_{L/R}^<(E)G^>(E) - \Sigma_{L/R}^>(E)G^<(E)], \quad (1)$$

where subscripts L/R indicate left or right lead. The NEGF $G^{\gtrless}$ are given in terms of the retarded and advanced Green's functions,

$$G^{\gtrless}(E) = G^R(E)[\Sigma_L^{\gtrless}(E) + \Sigma_R^{\gtrless}(E) + \Sigma_{e\text{-}p}^{\gtrless}(E)]G^A(E). \quad (2)$$

Here, $\Sigma_{L/R}^{\gtrless}(E)$ is the self-energy describing charge injection from the left/right leads[15] and $\Sigma_{e\text{-}p}^{\gtrless}(E)$ is the self-energy due to e-p interactions.[21]

Using the lowest-order Feynman diagrams for the e-p self-energy,[22] at zero temperature (the phonon occupation numbers $N_\nu = 0$) the total current can be written in terms of transmission functions as a sum of elastic and inelastic contributions,

$$I_{L/R} = I_{L/R}^{el} + I_{L/R}^{inel} = \frac{e}{h} \int dE (T_{L/R}^{el} + T_{L/R}^{inel})(f_{L/R} - f_{R/L}), \quad (3)$$

where the elastic transmission is obtained from Green's functions via the Fisher-Lee relationship,[23]

$$T_{L/R}^{el} = \mathrm{Tr}[\Gamma_{L/R}G^R\Gamma_{R/L}G^A]. \quad (4)$$

Here, $f_{L/R}$ are the Fermi functions of the leads and $\Gamma_{L/R}$ are the linewidth functions describing the coupling between the scattering region and leads. Note that although $T_{L/R}^{el}$ is called "elastic," it includes phonons through the Green's function. The inelastic transmission function can be written in a similar manner,
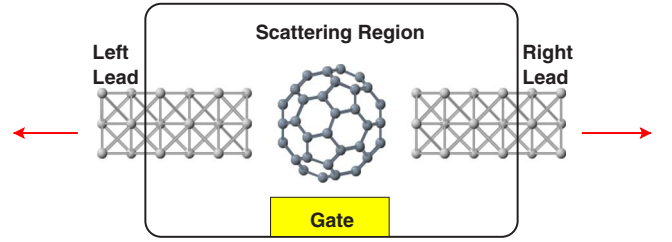
FIG. 1. (Color online) Schematic plot of the Al-C_{60}-Al tunneling junction. The scattering region of the device includes the molecule and four layers of the lead atoms.

$$T_{L/R}^{inel} = \mathrm{Tr}[\Gamma_{L/R}G^R\Gamma_{e\text{-}p,R/L}G^A], \quad (5)$$

where $\Gamma_{e\text{-}p} = \Gamma_{e\text{-}p,L} + \Gamma_{e\text{-}p,R}$ is the linewidth function due to e-p interactions. These functions are calculated by standard NEGF theory.[24] We emphasize that in our theory, the electronic Hamiltonian is self-consistently renormalized by nonequilibrium phonons, although only first-order phonon processes are included in the self-consistent numerics. The solution of the inelastic NEGF-DFT equations is implemented in our numerical package MCDCAL.[15] In what follows, we use localized atomic orbitals as a basis set and the nonlocal pseudopotentials to treat atomic cores.

To investigate e-p effects in quantum transport, we now turn to the Al(100)-C_{60}-Al(100) MTJ shown in Fig. [1]. With the lead-lead separation at 12.2 Å, C_{60} is well bonded to the leads so that Coulomb blockade can be neglected. Total-energy geometrical relaxation of the molecule plus two nearest lead layers is carried out by DFT (Refs. [15] and [25]) at equilibrium. Significant charge transfer by more than two electrons from the Al leads to the LUMO of C_{60} is found, and transport is mediated by LUMO-derived molecular orbitals; these results are in agreement with previous studies.[25–27] As a further check, we calculate vibrational spectrum of an *isolated* C_{60}, and the obtained frequencies are within 10% of Raman and IR spectroscopy results.[28,29] When C_{60} is placed between the leads, rotational symmetry is broken and the lead-molecule interaction causes a slight change of geometry. As a result, we find that degeneracies of C_{60} vibrational modes are lifted and several low-frequency modes softened. The vibrational frequencies are found to range from 212 to 1590 cm^{-1} (26–200 meV).

Figure [2] plots total transmission function at zero bias versus energy in the presence of e-p interaction (dashed line), obtained by adding Eqs. [4] and [5]. This is to be compared with that of no e-p coupling (solid line). The sharp peak of the transmission near $E = 0.2$ eV, which is due to resonance mediated tunneling by one of the LUMO-derived states, is suppressed by e-p interaction and redshifted by ~50 meV toward the Fermi energy of the device. This is an unusually strong shift due to e-p coupling.

To shed light on this unusually large redshift of a transmission feature, we first project scattering states responsible for transmission near the Fermi energy onto the C_{60} molecular orbitals (MO's). These molecular orbitals are obtained by diagonalizing the submatrix corresponding to the C_{60} inside the full NEGF-DFT Hamiltonian of the device. The MO's
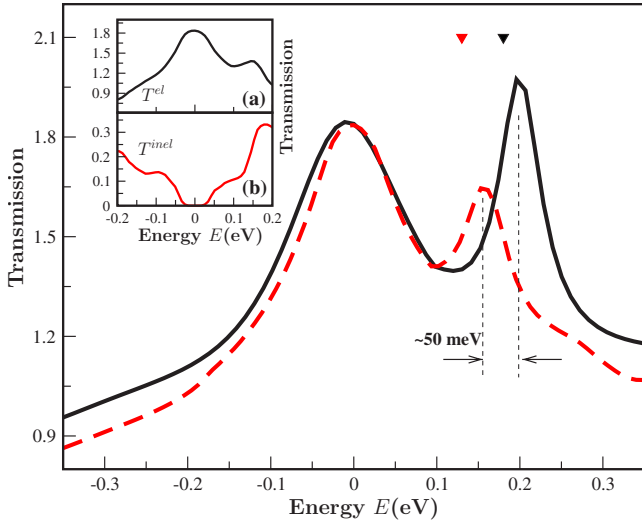
FIG. 2. (Color online) Transmission versus energy with no e-p coupling (solid line) and with e-p coupling (dashed line) ($E=0$ corresponds to the Fermi energy). The sharp transmission peak near $E=0.2$ eV is shifted toward the Fermi energy due to the strong e-p coupling. The LUMO-derived states with and without e-p coupling are schematically shown with the triangles. Inset: (a) Elastic and (b) inelastic components of the total transmission function (with e-p coupling).

FIG. 3. (Color online) (a) Derivative of the inelastic transmission function with respect to energy. (b). The e-p coupling strength computed from LUMO orbitals near the Fermi level of the device versus frequency of the C_{60} vibrational modes.

calculated this way describe the molecule interacting with the open environment and can be referred as "renormalized molecular orbitals" (RMO's).[30] In general, the projection is defined as

$$\hat{P}_{RMO}\Psi_{sc}(\epsilon,k) = \sum_i a_i(\epsilon,k)|RMO_i\rangle, \qquad (6)$$

where $\Psi_{sc}(\epsilon,k)$ is the scattering state of the tunneling junction with energy ϵ and wave number k. Here, the summation is over the target renormalized molecular orbitals. One can well consider that $\Psi_{sc}(\epsilon,k)$ is a linear combination of these RMO's weighted by the coefficients $a_i(\epsilon,k)$. We find that only three LUMO-derived states contribute to tunneling near the Fermi level. It appears that the molecular orbitals are renormalized not only by the interaction with the electrodes but also by e-p interaction. Indeed, comparing the energy of LUMO-derived states with and without e-p coupling, we find these states to be redshifted in energy, as shown in Fig. 2 with the triangles. Importantly, this effect results from the self-consistency between the electron charge density and the electronic Hamiltonian. This is a key feature of our theory: keeping these variables self-consistent yields the correct treatment of molecular orbitals. Next, we plot the derivative of the inelastic transmission T^{inel} with respect to energy in Fig. 3 (upper panel), and compare it with the e-p coupling strength (lower panel) which is defined as

$$\lambda_j^\nu \equiv \frac{\langle LUMO_j|g^\nu|LUMO_j\rangle}{\hbar\omega_\nu}, \qquad (7)$$

where g^ν is the e-p coupling matrix and $LUMO_j$ is one of three LUMO-derived orbitals responsible for transmission.

This comparison allows us to observe all features in the transmission which correspond to excitations of the vibrational modes. Indeed, the quantity dT^{inel}/dE gives a good measure to IETS spectra d^2I/dV_b^2 and it clearly reveals which phonon modes contribute to transport. The total transmission, on the other hand, may have a cancellation between elastic and inelastic contributions due to interference, as shown in the inset of Fig. 2.

Comparing the upper and lower panels of Fig. 3, we observe that features in dT^{inel}/dE coincide rather well with phonon frequencies of the modes that strongly couple to LUMO-derived states (i.e., those modes with high values of λ_j). Therefore, the transmission and consequently the current and conductance undergo significant changes due to resonances mediated by the MO's. Figure 3 indicates that among the 174 available vibrational modes included in our calculation, only a few are strongly coupled to transport. Figure 3 shows that modes contributing most to transport are those with H_g symmetry. These modes are also Raman active. This finding is consistent with recent IETS experiments of Pascual *et al.*[5] on single C_{60} molecules adsorbed on Ag(110) substrate. In particular, Pascual *et al.*[5] assigned a large d^2I/dV^2 peak at $eV_b=54$ meV to the $H_g(\omega_2)$ mode. For our system, this mode also gives large e-p coupling, as shown in Fig. 3. In addition, our results lend strong support to the IETS experiment of Pradhan *et al.*,[6] suggesting that most of the eight H_g and $A_g(\omega_1)$ modes are strongly coupled to transport (see Fig. 3). An exception is that we could not identify $A_g(\omega_1)$ mode for our device, which is likely due to its symmetry and strong interaction with the electrodes. Indeed, experiments indicate that vibrational spectra depend on the substrate material as well as on the orientation of the C_{60} cage with respect to the substrate.

To understand why these modes couple more strongly than others to transport, we investigate the spatial extent of the MO's participating in resonance tunneling. We find that vibrational modes with high e-p coupling involve the motion
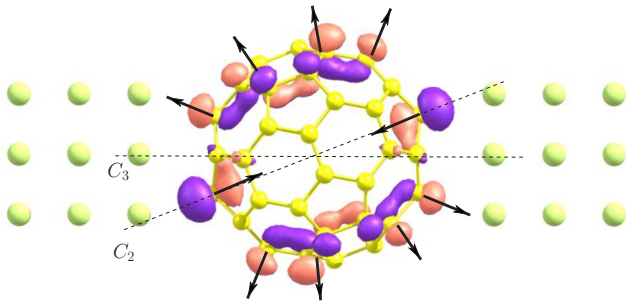
FIG. 4. (Color online) Isosurface plot of one LUMO-derived orbital. The eigenvectors of the $H_g(\omega_1)$ vibrational mode with frequency $\hbar\omega \approx 212$ cm^{-1} are shown by the arrows. The molecule is "stretched" along the C_2 symmetry axis due to this mode.

of those atoms on which the LUMO-derived orbitals are localized. An isosurface plot of one of the LUMO-derived orbitals, along with the eigenvectors of the dynamical matrix corresponding to $H_g(\omega_1)$ mode, is shown in Fig. 4. This particular vibrational mode involves "stretching" of the C_{60} molecule along its C_2 symmetry axis. Consequently, this motion effectively changes an overlap between the molecule and the electrodes, thus making this vibrational mode affect transmission significantly.

In conclusion, we have developed *ab initio* theory of IETS and applied it to the metal-C_{60}-metal MTJ. Our results confirm tentative mode assignment of recent IETS experiments on C_{60} MTJ's. We find that the metal Fermi-level realignment to the C_{60} LUMO results in the LUMO mediated transport which is very strongly affected by e-p coupling. The physics behind the large e-p effect for this system is that the LUMO wave functions are localized on atoms producing relevant vibrational modes. Furthermore, the e-p interaction causes the renormalization of the molecular orbitals, resulting in the significant redshift of the transmission features. The self-consistency between the charge density, Green's function, and Hamiltonian in the presence of the e-p interaction is found essential for capturing this nonequilibrium effect correctly.

[1] D. A. Cass, H. L. Strauss, and P. K. Hansma, Science **192**, 1128 (1976).

[2] B. C. Stipe, M. A. Rezaei, and W. Ho, Science **280**, 1732 (1998).

[3] S. K. Khanna and J. Lambe, Science **220**, 1345 (1983).

[4] J. I. Pascual, N. Lorente, Z. Song, H. Conrad, and H.-P. Rust, Nature (London) **423**, 525 (2003).

[5] J. I. Pascual, J. Gomez-Herrero, D. Sanchez-Portal, and H.-P. Rust, J. Chem. Phys. **117**, 9531 (2002).

[6] N. A. Pradhan, N. Liu, and W. Ho, J. Phys. Chem. **109**, 8513 (2005).

[7] D.-H. Chae, J. F. Berry, S. Jung, F. A. Cotton, C. A. Murillo, and Z. Yao, Nano Lett. **6**, 165 (2006).

[8] N. Lorente and M. Persson, Phys. Rev. Lett. **85**, 2997 (2000).

[9] W. Wang, T. Lee, I. Kretzschmar, and M. A. Reed, Nano Lett. **4**, 643 (2004).

[10] A. Troisi, M. A. Ratner, and A. Nitzan, J. Chem. Phys. **118**, 6072 (2003).

[11] M. Galperin, M. Ratner, and A. Nitzan, J. Chem. Phys. **121**, 11965 (2004).

[12] Y. Asai, Phys. Rev. Lett. **93**, 246102 (2004).

[13] T. Frederiksen, M. Brandbyge, N. Lorente, and A.-P. Jauho, Phys. Rev. Lett. **93**, 256601 (2004).

[14] M. Paulson, T. Frederiksen, and M. Brandbyge, Nano Lett. **6**, 258 (2006).

[15] J. Taylor, H. Guo, and J. Wang, Phys. Rev. B **63**, 245407 (2001).

[16] N. Sergueev, D. Roubtsov, and H. Guo, Phys. Rev. Lett. **95**, 146803 (2005).

[17] H. Park, J. Park, A. K. L. Lim, E. H. Anderson, A. P. Alivisatos, and P. L. McEuen, Nature (London) **407**, 57 (2000).

[18] K. Prassides, J. Tomkinsonb, C. Christides, M. J. Rosseinsky, D. W. Murphy, and R. C. Haddon, Nature (London) **354**, 462 (1991).

[19] S. Datta, *Electronic Transport in Mesoscopic Systems* (Cambridge University Press, Cambridge, 1995).

[20] T. N. Todorov, J. Hoekstra, and A. P. Sutton, Philos. Mag. B **80**, 421 (2000).

[21] N. Sergueev, Ph.D. thesis, McGill University, Montreal, Canada, 2005.

[22] G. D. Mahan, *Many-Particle, Physics*, 2nd ed. (Plenum, New York, 1990).

[23] D. S. Fisher and P. A. Lee, Phys. Rev. B **23**, 6851 (1981).

[24] H. Haug and A.-P. Jauho, *Quantum Kinetics in Transport and Optics of Semiconductors* (Springer, New York, 1996).

[25] J. Taylor, H. Guo, and J. Wang, Phys. Rev. B **63**, 121104(R) (2001).

[26] J. J. Palacios, A. J. Pérez-Jiménez, E. Louis, and J. A. Vergés, Phys. Rev. B **64**, 115411 (2001).

[27] S. Alavi and T. Seideman, J. Chem. Phys. **115**, 1882 (2001).

[28] M. G. Mitch, S. J. Chase, and J. S. Lannin, Phys. Rev. Lett. **68**, 883 (1992).

[29] D. S. Bethune *et al.*, Chem. Phys. Lett. **179**, 181 (1991).

[30] The procedure of calculating these renormalized MO's can be found in B. Larade, J. Taylor, Q. R. Zheng, H. Mehrez, P. Pomorski, and H. Guo, Phys. Rev. B **64**, 195402 (2001).